Structures 68 (2024) 107138

Contents lists available at ScienceDirect

Structures

journal homepage: www.elsevier.com/locate/structures

Predicting the non-linear behaviour of cross laminated timber shearwalls with cut-out openings

Martina Sciomenta [a,*], Riccardo Fanti [b], Ghasan Doudak [c], Andrea Polastri [b], Daniele Casagrande [d]

[a] Department of Civil, Architecture and Building and Environmental Engineering, University of L'Aquila, Via Giovanni Gronchi 18, 67100 L'Aquila, Italy
[b] Institute of Bioeconomy, National Research Council of Italy, via Francesco Biasi, 75, 38098 San Michele all'Adige, Trento, Italy
[c] Faculty of Civil Engineering, University of Ottawa, 161 Louis-Pasteur Pièce, Ottawa, ON K1N 6N5, Canada
[d] Department of Civil, Environmental and Mechanical Engineering, University of Trento, Via Mesiano 77, 38123 Trento, Italy

ARTICLE INFO

Keywords:
CLT
Openings
Modelling
Non-linear analyses
Stiffness
Lintels

ABSTRACT

The behaviour and failure mode expected in Cross Laminated Timber (CLT) shearwalls when either window or door openings are incorporated into the shearwalls may be considerably different than that of shearwalls without openings. Despite clear theoretical and experimental evidence of the possible occurrence of significant increase in the deformation contribution of the CLT panels and induce high stress concentrations around openings, limited studies have been conducted on the effect of crack propagation in CLT shearwalls with cut openings. The current study presents two modelling techniques to account for the crack propagation around openings, through concentrated plastic hinge (PHM) and continuous post-elastic (CPEM) models. The proposed models are validated using available experimental results obtained from six full-scale shearwalls in the literature while input parameters, such as the mechanical properties of the CLT panels, are obtained, in part, from component-level experimental investigation on CLT beams conducted by the authors as part of the current study. The impact and advantages of accurately predicting the non-linear behaviour of the CLT panels are investigated through a numerical analysis on a case-study representing a multi-storey shearwall with multiple openings. The results showed the inability of elastic models to predict the inelastic behaviour in the CLT shearwall after the crack opening, and this the study recommends the inclusion of stress redistribution near crack openings and subsequent inelastic behaviour in the analysis.

1. Background and literature review

1.1. Introduction

Strength capacity and deformation of Cross Laminated Timber (CLT) shearwalls with no openings are primarily governed by the behaviour of the mechanical anchors used to connect the shearwalls to its base or vertical joints connecting CLT panels together [1,2]. A considerably different behaviour and failure mode may be expected when either window or door openings are incorporated into the shearwalls. The openings may result in a significant increase in the deformation contribution of the CLT panels and induce high stress concentrations around openings, potentially leading to premature and undesired brittle failure modes. This is particularly plausible when openings are cut directly out of the CLT panels, resulting in structural continuity between lintel and/or parapet elements and the wall segments (Fig. 1a). Alternatively, openings can be constructed by assembling the individual elements in the wall by means of connections designed primarily to transfer the shear load from the lintel to the wall segments (e.g. by notching the wall segments and using dowel-type fasteners to join the two elements); however, such joints are not capable of providing any significant moment continuity (Fig. 1b).

The structural continuity and the interaction between lintel and parapet beams and wall segments in shear-wall with cut-out openings produce a shearwall behaviour that is much different from that of cantilever beams. This behaviour leads to heightened complexity in the prediction of mechanical behaviour of the shearwall since stress concentrations around openings and corresponding failure modes in the

* Corresponding author.
E-mail addresses: martina.sciomenta@univaq.it (M. Sciomenta), riccardo.fanti@ibe.cnr.it (R. Fanti), gdoudak@uottawa.ca (G. Doudak), andrea.polastri@ibe.cnr.it (A. Polastri), daniele.casagrande@unitn.it (D. Casagrande).

https://doi.org/10.1016/j.istruc.2024.107138
Received 17 January 2024; Received in revised form 24 June 2024; Accepted 21 August 2024
Available online 30 August 2024

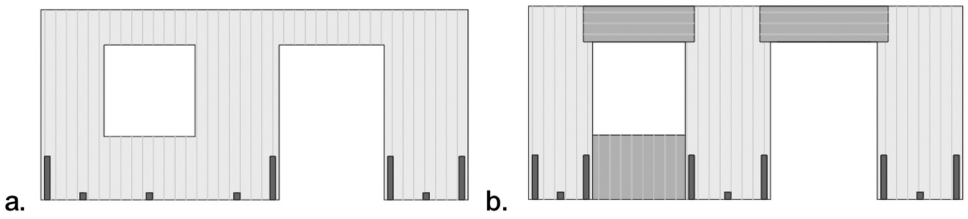

Fig. 1. CLT shearwalls with cut-out openings (a); CLT shearwalls where openings are obtained by assembling separated elements (b).

panel have to be carefully considered in the analysis model. Ignoring the interaction between various wall elements, for the purpose of simplifying the analysis and design method, could yield a significant reduction in design efficiency, especially for multi-storey lateral load resisting systems. Studies have shown that both strength and stiffness of shearwalls with cut-out openings are significantly higher than those obtained in assembled shearwalls (e.g., [17]).

Furthermore, an accurate prediction of the brittle failure modes in the panel is essential when CLT shearwalls are designed in seismic prone areas, where a capacity-based design approach is typically adopted to protect brittle failure modes in the panels and ensure yielding and energy dissipation in connections.

Research conducted on shearwalls with cut openings has been quite limited, but valuable information is available in literature on their mechanical behaviour. The following sections discuss the available literature on studies related to experimental testing, numerical modelling and introduces the theory relevant to this paper on crack propagation in timber elements.

1.2. Experimental studies on CLT shearwalls with openings

Ceccotti et al. [3] carried out an experimental test on a CLT shearwall with single door opening. The study reported that the CLT panels behaved elastically, and the failure mode was related to the mechanical anchors used to connect the shearwall to the foundation. Dujic et al. [4] reported on cyclic tests conducted on two single-storey shearwalls, each with a door and window opening. A ductile failure mode of the mechanical anchors was attained, with no crack opening observed in the panels. Similar outcome was reported by Popovski et al. [5] based on a cyclic test of a single-storey CLT shearwall with a door and a window opening, anchored to the foundation by means of angle brackets typically used for light-frame shearwalls. Popovski et al. [6] investigated a full-scale 2-storey CLT structure under quasi-static cyclic load and observed cracks in the corner of a door opening in one of the wall panels at the first storey. It was found that the global behaviour was primarily dominated by a combination of sliding and uplift of the angle brackets at the first storey. Yasamura et al. [7] investigated the mechanical performance of a two-storey CLT building made with two shearwalls at each storey with cut door and window openings. The observed failure mode was predominantly related to the uplift of the mechanical anchors due to rocking of the shearwalls, with some cracks detected at the corners of the openings.

Awad et al. [8] presented an experimental campaign on single-storey CLT shearwalls with either single or double openings. The results from the cyclic tests showed that failure in CLT panels occurred at the upper corner of the opening in almost all specimens, resulting in brittle failure mode of the shearwalls. Mestar et al. [9] investigated five shearwalls with either door or window openings with the aim to study the walls' rocking kinematic behaviour. A single centre of rotation, for the entire wall, was observed for the shearwalls consisting of window opening or door opening with stiff lintels. A kinematic mode, characterized by one centre of rotation for each wall segment, was achieved for the shearwall with door opening and slender lintel. For such wall configurations, crack opening and propagation were observed. Casagrande et al. [10] conducted monotonic tests on six CLT shearwalls with single cut-out door or window openings with the aim to investigate the geometrical and mechanical properties of the shearwall that could induce brittle failure mode in the CLT panel. The study reported crack opening and propagation in two of the four shearwalls with door openings. Isoda et al. [59] investigated the propagation of cracks around the corners in CLT shear-walls with cut-out openings through experimental tests on L- and T-shape specimens. Bending and rolling shear failures were observed in the lintel beam. The study also reported that the beam theory (i.e. strain distribution is not linear) cannot be adopted for the analysis of mechanical behaviour of such elements.

1.3. Numerical studies on CLT shearwalls with openings

Early development in numerical studies on CLT shearwalls with cut openings mainly focused on the determination of stiffness and strength reduction factors which take into account the geometrical dimensions of openings [11,12].

A similar approach was adopted by Shahnewaz et al. [13] to investigate the influence of the shape and dimension of the openings on the shearwall capacity and stiffness. In these studies, the CLT panels were modelled by means of orthotropic homogenous 2D shell elements characterized by linear-elastic material behaviour, using effective values for the modulus of elasticity and shear modulus. The mechanical anchors were modelled by means of bi-directional non-linear link elements.

Homogenous 2D shell elements, characterized by linear-elastic behaviour were also adopted by Fragiacomo et al. [14] to perform non-linear static analysis of a 3-storey CLT building. Link elements characterized by the non-linear behaviour obtained by experimental tests were adopted for the modelling of connections. Pai et al. [15] investigated force transfer around openings, while Casagrande et al. [16] studied the location and distribution of axial and shear internal forces in relevant sections of the CLT shearwall panels with openings. Several studies presented numerical predictions of the behaviour of CLT shearwalls with cut openings, tested experimentally under quasi-static monotonic or cyclic loading [7–10].

The adopted models differ from one-another mainly in the assumptions related to the implementation of the non-linear behavioural characteristics assigned to the mechanical anchors, including uni- vs bi-directional behaviour and tri-linear vs multi-linear behaviour; however, analogous approaches were used for the prediction of failure modes in the CLT panels. Since panels were modelled using linear-elastic material, a step-by-step verification of either internal stresses or internal forces per unit length in the shell elements was undertaken. The values obtained from the analyses were compared with the mean resistance values in the panel obtained from the experimental tests on isolated CLT members (i.e. small panels or beams). The same modelling strategy and failure criterion was adopted for CLT panels by Khajehpour et al. [17] in order to numerically investigate the influence of construction techniques of opening on the strength capacity and stiffness of multi-storey shearwalls.

Mestar et al. [18] and Casagrande et al. [19] proposed an equivalent frame model as an alternative to 2D shell elements for the analysis of shearwalls with cut openings. Lintel, parapet and wall segments were modelled by means of macro-element represented by horizontal and

vertical 1-D frame elements, with rectangular cross-section. Linear-elastic behaviour was assumed for the flexible parts of the macro-elements. A step-by-step verification procedure including axial load, shear load, and bending moment was conducted in the frame element in order to determine possible failure modes in the CLT panels. D'Arenzo [60] presented an analytical methodology to predict the lateral displacement of CLT shear-walls with a single door or window opening. The presented model is capable of considering two different rocking kinematic modes, namely one or two centre of rotations. Ruggeri et al. [61] conducted a parametrical study to investigate the interaction between the floor-to-wall connections and lintel elements on the mechanical behaviour of CLT shear-walls with cut-out openings. The results showed that such connections may have a significant role in the response of the shear-walls, while out-of-plane bending stiffness of the CLT floor panel has a negligible effect.

1.4. Crack propagation modeling in timber members

Linear elastic fracture mechanics (LEFM) deals with the initiation and propagation of cracks in elastic bodies [20–22]. In general, two different analytical techniques can be used to approach crack propagation problems in LEFM, namely stress intensity criterion and energy criterion. The former is based on the definition of a stress intensity factor, while the latter focusses on the energy released during the propagation of a pre-existing crack (i.e., compliance method). In the energy approach, the material is characterised by a corresponding critical energy release rate, G_c, or critical stress intensity factor, K_c, which characterizes the material's resistance to brittle fracture [23].

Timber is usually defined as cylindrically orthotropic material with axes of material symmetry corresponding to longitudinal (L), radial (R) and transversal (T) directions. Two assumptions are typically made concerning wood's behavior, in order to extend the basic LEFM principles: *i)* the specimen is taken a sufficient distance from the tree center such that the curvature of the growth rings can be ignored and rectilinearly orthotropic material behaviour can be assumed, and *ii)* timber behaves as a brittle solid, which is a reasonable assumption when the moisture content is sufficiently low [24].

For some complex-shaped structures with arbitrary crack front, the analytical definition of the stress intensity factors is difficult to achieve especially as closed-form solution, and therefore numerical methods, such as finite element analysis, have been extensively developed. Virtual Crack Closure Technique (VCCT) and Cohesive Zone Model (CZM) are often used for this purpose. These techniques have been successfully implemented in research involving crack formation in notched beams [25,26]. They have also been used to simulate bonded joint damage onset and growth [27,28], and to investigate the splitting strength of timber connections [29].

Other research related to cracks in glued timber members have been carried out using 3D Non-Linear Fracture Mechanic (NLFM) models [30,31]. The main aim of these analyses was to highlight the fracture propagation related to finger-joints strength [32], glued-in rods [33], and beams with holes [34]. The models were capable of accounting for defects such as fibre bridging along the crack and softening ahead of the crack tip.

The extended finite element method (XFEM) alleviates the shortcomings associated with meshing crack surfaces. This method assesses for the presence of discontinuities in a material by special enriched functions in conjunction with additional degrees of freedom. The XFEM is a well-established technique that does not require prior knowledge and determination of the crack path and is available with 2D and 3D models for LEFM as well NLFM methods. This method has been successfully utilized to model steel[35], concrete[36] and composites [37].

Qui et al. [38] developed XFEM-based models to simulate the crack propagation behaviour of wood in curved glulam beams. Crack initiation, propagation and failure load and patters obtained from a 3D numerical simulation were compared with full-size bending tests on beams, and the suitability of XFEM was established. Other studies on glulam beams were carried out by Kováčiková et al. [39] and Tapia and Aicher [40], where the XFEM method was used to simulate the tensile failure in timber boards and finger-joints in a glulam. Habite et al. [41] investigated the moisture-induced crack propagation in dowelled connection in glulam elements. Gebhardt and Kaliske [42] adopted the XFEM modelling technique to describe the brittle failures of wood using stress-based failure criterion predicated on multi-surface formulation.

1.5. Summary and contribution

Review of the available literature on the numerical modelling of CLT shearwalls with cut openings highlights the consensus to assume linear-elastic behaviour of CLT panels. However, results from experimental investigations conducted at both wall and building levels seem to indicate that crack propagation around openings may not always cause an abrupt brittle failure in the tested system, leading to the ultimate failure being primarily related to the connections, even in cases where panel local strength capacity is exceeded. In other words, shearwalls with cut openings have demonstrated the capacity to undergo significant lateral displacement beyond crack opening in the CLT panel. As a result, although the majority of numerical analyses that adopts linear-elastic behaviour of CLT panels showed a reasonable match in terms of strength capacity and stiffness with experimental results, there is a need to establish better understanding of the behaviour of CLT shearwalls after the occurrence of the crack.

The current study aims to provide adequate prediction of the CLT shearwall behaviour beyond crack initiation. A proposal for the numerical prediction of the mechanical behaviour of CLT shearwalls with cut openings is presented through FE models capable of considering the non-linear behaviour of CLT panels. Two different types of modelling techniques are defined to account for the crack propagation around openings. The proposed models are validated using available experimental results obtained from full-scale shearwalls in the literature while input parameters, such as the mechanical properties of the CLT panels, are obtained, in part, from component-level experimental investigation on CLT beams conducted by the authors as part of the current study. The impact and advantages of accurately predicting the non-linear behaviour of the CLT panels are investigated and demonstrated through the analysis of a case-study representing a multi-storey shearwall with multiple openings.

2. Proposal for the numerical prediction of shearwalls with cut-out openings

In this section, two modelling techniques are proposed for the numerical prediction of the non-linear behaviour of CLT shearwalls with cut openings. The proposed approaches are capable of analysing and incorporating the opening and propagations of cracks around the openings. The two models have been implemented in SAP2000 [45] and ABAQUS [46] software packages by introducing novel and simplified methodologies in the analysis of crack openings and propagation in CLT shearwall through a concentrated plastic hinge (PHM) and continuous post-elastic (CPEM) models, respectively. The modelling techniques were implemented in two different software, primarily due to the capabilities of those programs. ABAQUS has the capability to implement fracture mechanics formulation for crack initiation and propagation, while the procedure implemented in SAP is simpler (i.e., designer friendly), done due to the rigid link capability.

2.1. Description of proposed finite element models

2.1.1. Concentrated plastic hinge model (PHM)

Four-node quadrilateral homogenous shell elements, characterized by the same thickness as that of the wall, are adopted to model the CLT panels. Effective values of the modulus of elasticity along the vertical,

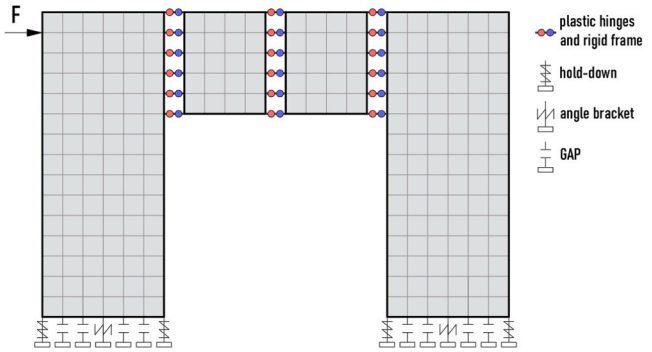

Fig. 2. Concentrated plastic hinge model (PHM).

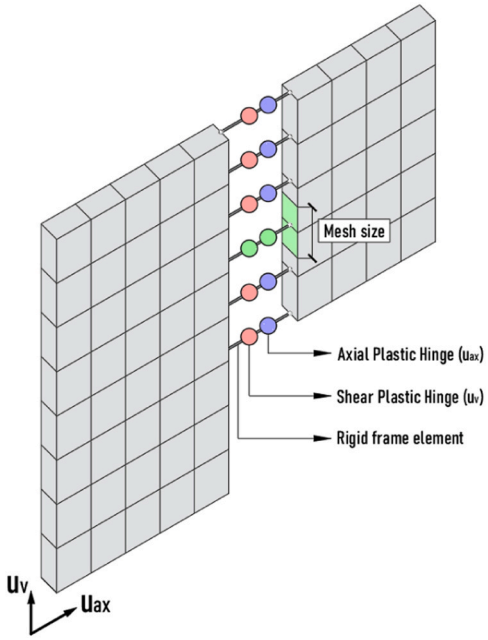

Fig. 3. Concentrated plastic hinges.

$E_{eff,v}$ (Eq. 1) and horizontal, $E_{eff,h}$ (Eq. 2) directions, as well as the in-plane shear modulus, G_{eff} (Eq. 3) are selected to represent the elastic orthotropic material behaviour, as presented by Bogensperger et al. [43] and Brandner et al. [44].

$$E_{eff,v} = \frac{E \bullet t_v}{t_{tot}} \tag{1}$$

$$E_{eff,h} = \frac{E \bullet t_h}{t_{tot}} \tag{2}$$

$$G_{eff} = \frac{G}{1 + 6 \bullet \alpha_T \bullet \left(\frac{t_{mean}}{w_b}\right)^2} \tag{3}$$

where E is the elastic modulus parallel to the grain of boards, t_{tot} the total thickness of the CLT panel, t_v and t_h are the total thickness of the vertical and horizontal layers, respectively, G is the in-plane shear modulus of boards, t_{mean} is the average thickness of boards, w_b is the width of boards or the distance between board's edge and notch and α_T is reported in Eq. 4.

$$\alpha_T = p_B \bullet \left(\frac{t_{mean}}{w_b}\right)^{q_B} \tag{4}$$

where q_B is equal to −0.79 and p_B and is equal to 0.53 and 0.43 for 3 and 5 layers CLT panel, respectively, as reported in [44].

In order to take into account the post-elastic behaviour of wood elements after crack opening, the shell elements at the end and mid-sections of the lintel and parapet segments are replaced with horizontal rigid frame elements, as outlined in Fig. 2. Two uncoupled axial and shear discrete plastic hinges are inserted at the mid-section of each frame element, in order to represent the concentrated post-elastic behavior along the horizontal and vertical direction, respectively, as shown in Fig. 3. Limiting the link elements to only the end and mid-sections of the lintel and parapet segments was based on observation from experimental tests on shear-walls with cut-out openings [9,10].

Rigid-perfectly plastic and rigid-brittle behaviour is assigned to the axial plastic hinge along the horizontal displacement (u_{ax}) to represent the compressive and tensile behaviour, respectively, while a symmetric rigid-brittle behaviour is assigned to the shear plastic hinge for the shear-vertical displacement (u_v).

The compressive $R_{ax,C}$, tensile $R_{ax,T}$ and shear R_v yield forces, which determine the activation of each plastic hinge, are calculated as expressed in Eqs. 5 to 7:

$$R_{ax,C} = s \bullet n_{ax,C,Rd} \tag{5}$$

$$R_{ax,T} = s \bullet n_{ax,T,Rd} \tag{6}$$

$$R_v = s \bullet n_{v,Rd} = s \bullet \min\begin{Bmatrix} n_{v,net,Rd} \\ n_{v,tor,Rd} \end{Bmatrix} \tag{7}$$

where $n_{ax,C,Rd}$ and $n_{ax,T,Rd}$ are the compressive and tensile strength per unit length of the CLT panel, respectively, $n_{v,Rd}$ is the shear strength per unit length, $n_{v,net,Rd}$ is the shear strength per unit length due to net shear mechanism, $n_{v,tor,Rd}$ is the shear strength per unit length due to torsional shear mechanism and s is the spacing between the rigid frame elements (for external frame elements the spacing is divided by two). Analytical expressions for the determination of compressive and tensile strength per unit length of the CLT panel can be calculated as the product of either the tensile or compressive strength of laminations and the lamination thickness along the horizontal and vertical direction as reported in [10]. It is noteworthy to mention that the first lamination (closest to the cut-out corner) is expected to be randomly reduced and this might lead to a local decrease in the torsional shear strength. Consequently, the outer links at the joints may be characterized by a torsional shear strength that is lower than the inner links.

One-joint and two-joint multi-linear link elements are used to model the hold-down and angle brackets at the ground and upper storeys, respectively, as shown in Fig. 2. Hold-downs and angle-brackets are characterized by bi-directional behaviour along the vertical-tensile and horizontal-shear directions. The contact between the CLT panels and the floor or ground below is simulated by means of rigid GAP (i.e. compression-only) elements. A multi-linear curve based on experimental testing is used to represent the behaviour of mechanical anchors. Vertical concentrated loads are applied at each node at the top of the shearwall, while horizontal loads (F) are applied at the top of each wall segments at every storey.

In order to include the non-linearity of materials representing the mechanical anchors and plastic hinges, non-linear static analyses are performed. Since axial and shear plastic hinges are uncoupled, the analysis is manually stopped when a single axial or shear plastic hinge attains its tensile $R_{ax,T}$ or shear R_v yield force, respectively. The corresponding frame element where one of the two plastic hinges yields is manually removed from the model, and a new analysis is run starting from the load condition reached in the previous analysis. The process persists until the failure of the entire shearwall is reached. It is noteworthy to mention that when an axial plastic hinge achieves its compressive yield force, the analysis is maintained since no crack opening is assumed under compression stresses, and the corresponding

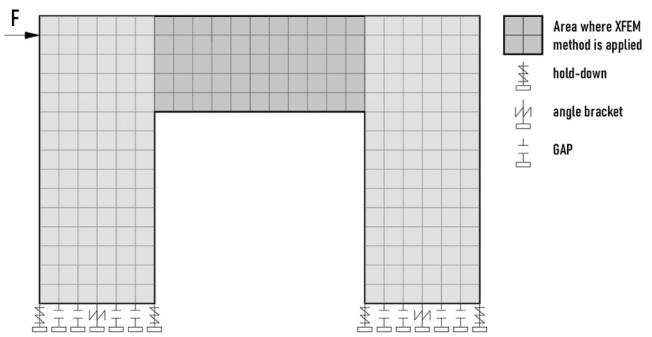

Fig. 4. Continuous post-elastic model (CPEM).

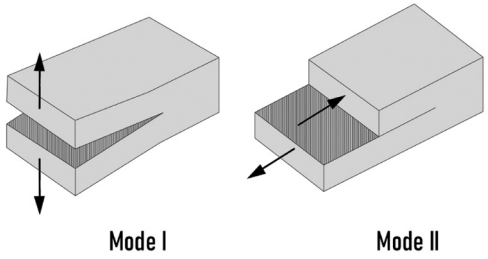

Fig. 5. failure along normal (mode I) and shear (mode II) direction of the crack.

shear plastic hinge can hence still transfer shear stresses.

2.1.2. Continuous post-elastic model (CPEM)

In this method, 2D shell element were used to model the CLT panel, using four-node CPS4R plane stress elements, with reduced integration [46]. The selection of this element presents a reasonable balance between accuracy and modelling efficiency, as demonstrated in the published literature [10,12,16].

The CLT panels were assigned elastic orthotropic material properties, with effective values of moduli of elasticity along the vertical, $E_{eff,v}$, and horizontal, $E_{eff,h}$, directions as well as in-plane shear modulus, G_{eff}, in accordance with the expressions presented in Eqs. 1 to 3, and consistent with those reported for the model described in Section 3.1.1. The occurrence of possible compressive damage and local failure mechanisms in wood is taken into account by the Hill criterion, which allows for different resistance values in the principal directions of the wood element.

The numerical simulations are carried out using the ABAQUS/Standard software package [46], in the form of quasi-static displacement time histories. The Standard solver is specifically chosen in order to use the XFEM method, which is capable of predicting crack initiation and propagation in the shearwall lintels. This is done along an arbitrary path by modeling the crack as an enriched feature. The aim of this modeling technique is to obtain estimates of the elastic and damaged conditions up to failure. The cohesive segment method was selected since it represents a more suitable damage modeling within the XFEM framework. This enables the definition of the cohesive behavior in terms of a traction-separation law, by specifying the damage properties in the material definitions.

In the developed model, the possibility for cracks to develop was limited to area around the lintels, as shown in Fig. 4. This is consistent with observations made in the experimental studies on shear-walls with cut-out openings [9,10].

A stress-based damage initiation criterion (maximum nominal stress criterion - MAXS), and an energy-based evolution law are selected in order to study the crack detection using XFEM. To define the MAXS criterion, it is necessary to establish the nominal traction stress vector, as defined in Eq. 8. In 2D analyses, this stress vector consists of two components: normal stress component to the cracked surface (σ_n) and in-plane shear component (σ_s). Since the lintels are primarily subjected to bending and shear, the peak values of the nominal stresses, σ_n^0 and σ_s^0, are set equal to the effective bending strength $f_{m,h,eff}$ and the effective shear strength $f_{v,eff}$, as expressed in Eqs. 8 and 9, respectively.

$$f_{m,h,eff} = \frac{n_{ax,Rd}}{t_{tot}} \tag{8}$$

$$f_{v,eff} = \frac{\min(n_{v,net,Rd} : n_{v,tor,Rd})}{t_{tot}} \tag{9}$$

Damage is assumed to initiate when the maximum nominal stress ratio, as defined in Eq. 10, reaches a value of unity.

$$\max\left\{\frac{\sigma_n}{\sigma_n^0}, \frac{\sigma_s}{\sigma_s^0}\right\} = 1 \tag{10}$$

The Wu crack propagation criterion is defined to compute the equivalent fracture energy release rate [38]. In Abaqus, the criterion is implemented in terms of energy release rate as expressed in Eq. 11:

$$f = \frac{G_{equiv}}{G_{equivC}} = \left(\frac{G_I}{G_{IC}}\right)^{a_m} + \left(\frac{G_{II}}{G_{IIC}}\right)^{a_n} \geq 1 \tag{11}$$

where G_{equiv} is the equivalent strain energy release rate, which refer to the work done by the tension and its conjugate relative displacement in the normal and shear direction (G_I and G_{II}), respectively. G_{equivC} is the equivalent strain energy release rate which refers to the critical fracture energies required to cause failure in the normal and the shear directions, (G_{IC} and G_{IIC}), respectively (see Fig. 5). f indicates the status of the crack-tip node, where fracture is expected to occur when this factor reaches a value of unity. The empirical parameters, a_m and a_n, are assumed equal to $a_m = 0.5$ and $a_n = 1$, according to [38].

The mechanical connections were modelled in a manner consistent with that described in Section 3.1.1. The definition of non-linear behavior of springs is not directly supported in ABAQUS interface, and it was therefore defined by modifying the input file.

3. Model validation

3.1. Description of the tested shearwalls used in the validation

The validation of the proposed models is undertaken by comparing the results obtained from numerical models mimicking the behaviour of the shearwalls, as described in Section 3, with those from six full-scale shearwalls with cut-out openings available in literature. The experimental results were obtained from shearwalls published in five different experimental campaigns (Casagrande et al. [10]; Dujic et al. [4]; Ceccotti et al. [3]; Popovski et al. [5]; Mestar et al. [9]), and contained one (door) or two (door and window) openings.

Either three- or five-ply CLT panels were adopted for the shearwall specimens with a total panel thickness ranging between 85 and 100 mm. WHT620 Hold-downs [55] connected to the CLT panels with fifty-five 4x60mm ring shanked nails were adopted in the three shearwalls tested by Casagrande et al. [10] and Mestar et al. [9]), whereas HTT22 hold-down [56] connected to the panel with fourteen 4x60mm ring shanked nails was used in the shearwall tested by Ceccotti et al. [3]. ABR105 angle brackets [57] were used to connect to the CLT panel using ten 4x40mm ring shanked nails or 4.2x89mm spiral nails in the shearwalls tested by Duijic et al. [4] and Popovski et al. [5], respectively. AE116 angle brackets [57] with sixteen 4x60mm ring shanked nails were used to limit the sliding of the wall specimen tested by Ceccotti et al. [3], whereas blocking mechanism was adopted to fully prevent the sliding in the shearwalls tested by Mestar et al. [9] and Casagrande et al. [10].

The results, in terms of shearwall load-displacement curves, were used to compare with and validate the proposed numerical models, by

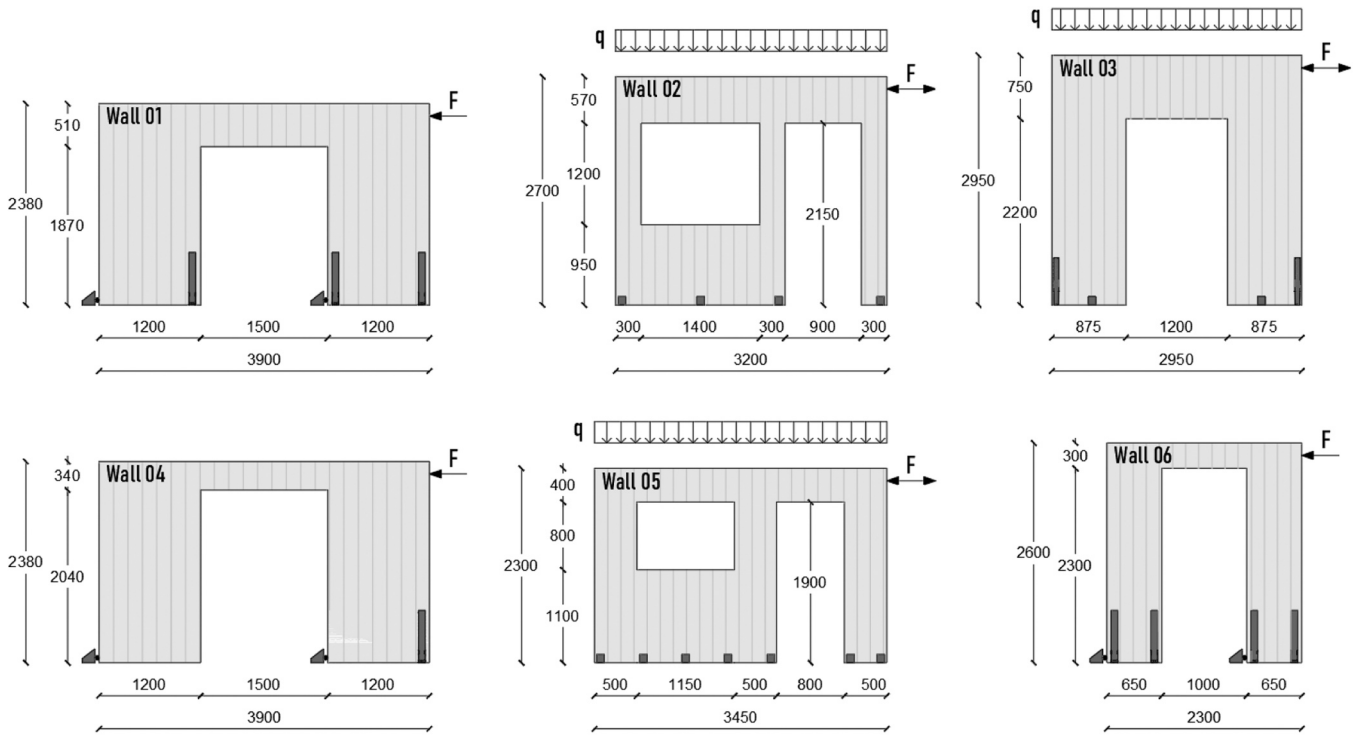

Fig. 6. Geometry of the tested shearwalls, reproduced from the literature. Wall 01 and 04 from [10]. Wall 02 from [4]. Wall 03 from [3]. Wall 05 from [5]. Wall 06 from [9].

Table 1
CLT panel layup, mechanical anchors and failure mode of tested shearwalls used for the validation.

Wall	Reference	CLT panel layup	Panel thickness t_{tot} [mm]	Hold-down	Angle brackets	Vertical load q [kN/m]	Load protocol	Failure mode
Wall 01	Casagrande et al.[10]	3-ply(30v−30 h−30v)	90	WHT620	Blocking mechanism	-	monotonic	CLT
Wall 02	Dujic et al.[4]	3-ply(30v−34 h−30v)	94	-	ABR105	15	cyclic	Angle bracket
Wall 03	Ceccotti et al.[3]	5-ply (17v−17 h−17v−17 h−17v)	85	HTT22	AE116	18,5	cyclic	Hold-down
Wall 04	Casagrande et al.[10]	5-ply (20v−20 h−20v−20 h−20v)	100	WHT620	Blocking mechanism	-	monotonic	CLT
Wall 05	Popovski et al.[5]	3-ply(30v−34 h−30v)	94	-	ABR105	20	cyclic	Angle bracket
Wall 06	Mestar et al.[9]	5-ply (17v−17 h−17v−17 h−17v)	85	WHT620	Blocking mechanism	-	monotonic	CLT

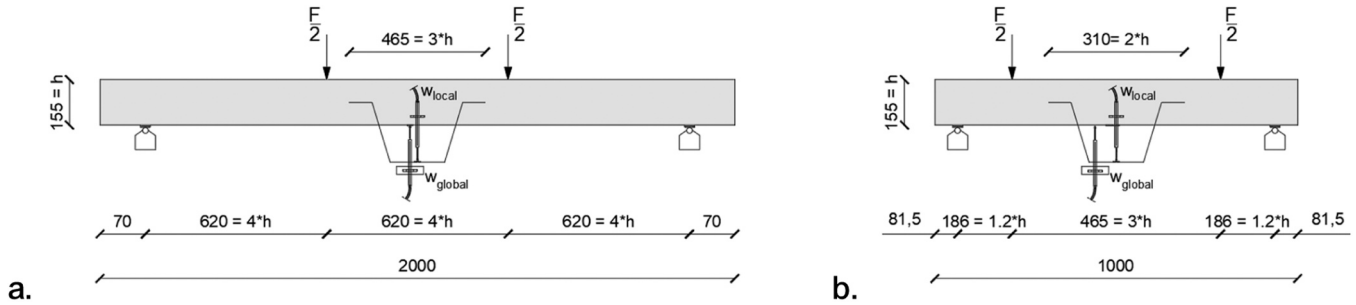

Fig. 7. Beam test setup with aim to obtain bending a), and shear failure b).

using consistent input parameters, such mechanical properties of the CLT panels and load-displacement curves of the mechanical anchors. These values were obtained from component-level tests conducted in isolation, in order to incorporate more precise input parameters into the numerical model and to minimize the variability usually associated with failure in the wood material and mechanical anchors. The mechanical properties of the WHT620 and HTT22 hold-downs with the same number of nails as those adopted in the shearwall tests were obtained from Casagrande et al. [10] and Gavric et al. [2], respectively. The behaviour of the ABR105 angle brackets in shear and tension were

Table 2
CLT beam specimens.

Beam ID	n. of test	Length [mm]	Orientation of outer laminations	t_h [mm]	t_v [mm]
B_L_L	3	2000	Horizontal	51	34
B_V_L	3	2000	Vertical	34	51
B_L_S	3	1000	Horizontal	51	34
B_V_S	3	1000	Vertical	34	51

obtained from Dujic et al. [4] and Shen et al. [47], while the load-displacement curves for the AE116 angle brackets were obtained from [2]. The geometrical dimensions of the shearwalls and the layout of the mechanical anchors used to prevent sliding and rocking of the walls are presented in Fig. 6. The CLT panel layup, type of mechanical anchors, magnitude of vertical load and the load protocol are reported in Table 1.

The mechanical properties of the CLT panels used to validate the model against the data from Wall 01 and Wall 04 (see Table 1) were obtained from experimental test results on CLT beams reported in Casagrande et al. [20], and they include modulus of elasticity as well as axial and in-plane shear strength of laminations. Similarly, the values of the modulus of elasticity of the CLT panels representing Wall 02 were obtained from experimental tests on small CLT panels reported in the study by Dujic et al. [4]. The same tests were also used for Wall 05, since the same CLT panel lay-up and manufacturer were used.

3.2. Experimental investigation of CLT beams

An experimental campaign was conducted as part of the current study to investigate CLT beams characterized by the same panel lay-up, wood species and manufacturer as those used in the full-scale shearwall tests of Wall 03 and Wall 06, as described in this section. This was motivated by the fact that no information was available on the mechanical properties of the 5-ply 85 mm thick CLT panels used in these walls.

The experimental study was conducted on twelve CLT beam specimens consisting of the same layup, number of plies (5), width of laminations (78 mm), wood species (spruce) and grade of lamination (C24), and manufactured according to ETA-06/0138 [58], as those used in the full-scale shearwall tests reported in Ceccotti et al. [3] and Mestar et al. [9]. The values of axial and in-plane shear strength of the laminations obtained from these tests were also used to augment the reference values for the Wall 02 and Wall 05, since CLT panels from those studies were from the same manufacturer and composed of the same wood species and grade as the ones tested in the current study, and parameters for the CLT panel tests reported Dujic et al. [4] were only limited to the modulus of elasticity. The height of all beam specimens, *h,* was equal to 155 mm, while the configurations consisted of two different lengths, equal to 2.0 m and 1.0 m, in order to promote bending and shear failure modes, respectively. Two different orientations of outer laminations were also selected, namely vertical and horizontal.

The test setup and boundary conditions for the beam tests are shown in Fig. 7. Each specimen was supported on steel rollers and loaded at the

Table 4
CLT mechanical properties adopted in numerical models.

Wall	E [MPa]	G [MPa]	$n_{ax,Rd}$ [kN/m]	$n_{v,Rd}$ [kN/m]
Wall 01	13411 from[10]	690 from[10]	1455 from[10]	273 from[10]
Wall 02	13158 from[4]	730 from[4]	1520 from Table 3	412 from Table 3
Wall 03	12246 from Table 3	500 from[58]	1520 from Table 3	412 from Table 3
Wall 04	13878 from[10]	690 from[10]	2008 from[10]	440 from[10]
Wall 05	13158 from[4]	730 from[4]	1520 from Table 3	412 from Table 3
Wall 06	12246 from Table 3	500 from[58]	1520 from Table 3	412 from Table 3

Fig. 8. CLT beam failure mode: a) bending, b) net shear, c) torsional shear.

Table 3
Mechanical parameters for tested CLT beams.

ID	F_{max} [kN]	E [MPa]	$n_{m,Rd}$ [kN/m]	$n_{v,Rd}$ [kN/m]	f_m [MPa]	f_v [MPa]	f_{tor} [MPa]	mode of failure
B_L_L_001	25.8	10630	1329	-	39.1	-	-	bending
B_L_L_002	28.1	12775	1448	-	42.6	-	-	bending
B_L_L_003	21.2	10631	1091	-	32.1	-	-	bending
B_V_L_001	17.1	11981	1319	-	38.8	-	-	bending
B_V_L_002	25.2	14480	1948	-	57.3	-	-	bending
B_V_L_003	26.9	12980	2084	-	61.3	-	-	bending
B_L_S_001	103.4	-	> 1601	500	> 47.1	> 14.7	6.5	torsional shear
B_L_S_002	87.4	-	> 1353	423	> 39.8	> 12.4	5.5	torsional shear
B_L_S_003	87.3	-	1350	> 422	39.7	> 12.4	> 5.4	bending
B_V_S_001	67.7	-	1574	> 328	46.3	> 9.6	> 4.2	bending
B_V_S_002	66.1	-	> 1537	320	> 45.2	9.4	> 4.1	net shear
B_V_S_003	84.0	-	> 1948	406	> 57.3	11.9	> 5.2	net shear
Average	-	**12246**	**1520**	**412**	**44.7**	**10.7**	**6.0**	
CoV		**12 %**	**22 %**	**18 %**	**22 %**	**17 %**	**12 %**	

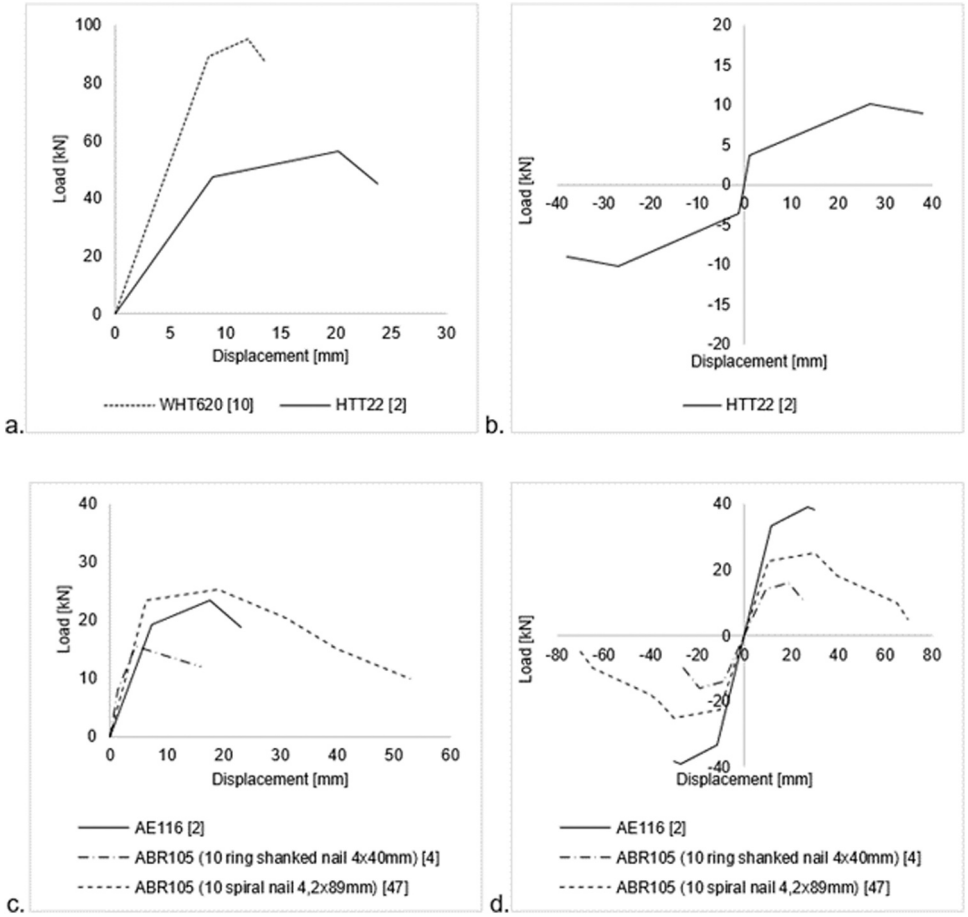

Fig. 9. Load displacement curves on Hold-down subjected to vertical-tensile (a) and horizontal-shear forces (b) and on angle-brackets subjected to vertical-tensile (c) and horizontal-shear forces (d).

one-third span points. The load was applied at a constant rate equal to 0.1 mm/s, according to EN408 [53], and continued until specimen failure. Two LVDTs, one on each side of the beam, were used to measure the total vertical deflection at the mid-span, while two other LVDTs measured the local relative displacement between the centre of the beam and another point within the zero-shear zone. Table 2 summarizes the lengths of the beam specimens and total thickness of lamination along the horizontal t_h and vertical t_v directions.

A bending failure mode was observed for all beams with length equal to 2.0 m. For the beams measuring 1.0 m in length and consisting of horizontal outer laminations, two specimens failed in torsional shear and one in bending. For beams with vertical laminations, two specimens failed in net shear and one in bending. Fig. 8 shows examples of the three failure modes that were observed in the CLT beams.

The local modulus of elasticity, E, of the laminations parallel to grain was determined from the beams with length equal to 2.0 m according to the formulation proposed in EN408 [53] without considering the shear deformation contribution, where the area moment of inertia, I_{eff}, is calculated according to Eq. 12.

$$I_{eff} = \frac{t_h \bullet h^3}{12} \tag{12}$$

The bending strength per unit length, $n_{m,Rd,}$ can be calculated as expressed in Eq. 13, assuming full composite action between longitudinal laminations. The shear strength per unit length, $n_{v,Rd}$ is determined based on Eq. 14 assuming a parabolic distribution of shear stresses along the gross section.

$$n_{m,Rd} = \frac{6}{h^2} \bullet \frac{F_{\max} \bullet a}{2} \tag{13}$$

$$n_{v,Rd} = \frac{3}{2} \bullet \frac{F_{\max}}{2 \bullet \mathrm{h}} \tag{14}$$

The bending strength, f_m and net shear strength, f_v are calculated based on Eqs. 15 to 16, respectively, taking into account only the contribution of horizontal layers, according to [62,63].

$$f_m = \frac{n_{m.Rd}}{t_h} = \frac{3 \bullet F_{\max} \bullet a}{t_h \bullet h^2} \tag{15}$$

$$f_v = \frac{n_{v,Rd}}{\min(t_h; t_v)} = \frac{3 \bullet F_{\max}}{4 \bullet \min(t_h; t_v) \bullet h} \tag{16}$$

where $F_{\max}$ is the maximum load obtained from testing, and a is the distance between load application point and support.

Flaig and Blaß (2013) presented a model to predict the torsional shear failure in CLT beams with horizontal outer lamination. This model was subsequently further developed by Danielsson and Serrano [64], Danielsson et al. [65], and Danielsson and Jeleč [66]. It should be noted however that this method cannot be directly implemented for all CLT beam lay-ups. The shear stresses between laminations, depend on where the horizontal layers are located in the beam. It is possible to adopt the analytical method presented by Danielsson and Serrano (2018) for 3-ply and 5-ply CLT beams with outer vertical laminations provided that, in the latter, the ratio between the thickness of the i-th vertical layer $t_{v,i}$ and the number of crossing areas $n_{CA,i}$ for the vertical layer under consideration is the same for all the three vertical layers. Since the beams

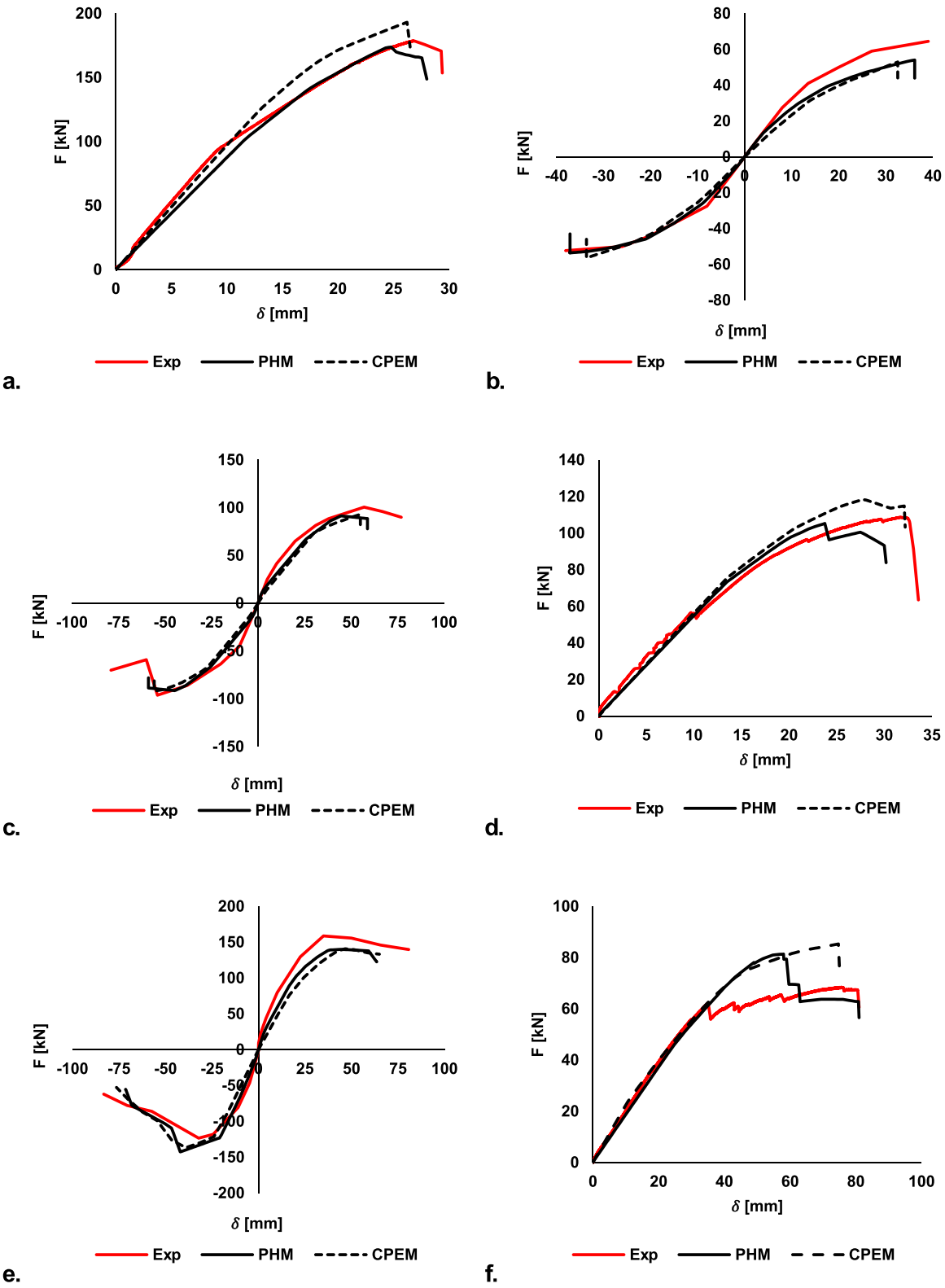

Fig. 10. Comparison between numerical models and experimental tests. a) Wall 01; b) Wall 02; c) Wall 03; d) Wall 04; e) Wall 05; f) Wall 06.

tested in this study do not meet such conditions, the torsional shear strength, f_{tor}, was determined based on Eq. 17, according to Andreolli et al. [48].

$$f_{tor} = \frac{3}{4}\frac{F_{max}}{w_b \bullet h} \tag{17}$$

The output results from the beam testing and the failure modes are reported in Table 3. It is noteworthy to mention that in the calculation of the average values and the Coefficients of Variations (CoVs) of each mechanical parameter, only the values related to the corresponding failure mode were used. The value corresponding to the observed failure mode is reported to reflect the strength of the beam while values for

Table 5
Comparison between numerical model and experimental tests.

	k [kN/mm]					F_{max} [kN]					mode of failure		
ID	test	CPEM	ε_{CPEM}	PHM	ε_{PHM}	test	CPEM	ε_{CPEM}	PHM	ε_{PHM}	test	CPEM	PHM
Wall 01	10.2	9.8	−4.4 %	8.7	−14.6 %	178.6	193.2	8.2 %	173.8	−2.7 %	CLT bending	CLT bending	CLT bending
Wall 02	3.4	2.3	−30.6 %	2.7	−19.1 %	64.5	52.9	−17.9 %	54.1	−16.2 %	anchor	anchor	anchor
Wall 03	3.1	2.4	−21.3 %	2.5	−19.4 %	100.6	92.9	−7.6 %	91.4	−9.2 %	anchor	anchor	anchor
Wall 04	5.5	5.6	3.4 %	5.4	−0.5 %	108.7	118.4	8.9 %	105.2	−3.2 %	CLT bending	CLT bending	CLT bending
Wall 05	7.0	4.7	−33.2 %	6.4	−8.9 %	158.6	140.8	−11.3 %	139.9	−11.8 %	anchor	anchor	anchor
Wall 06	1.9	2.0	2.5 %	1.9	−4.6 %	68.4	85.3	24.7 %	81.4	18.9 %	CLT bending	CLT bending	CLT bending

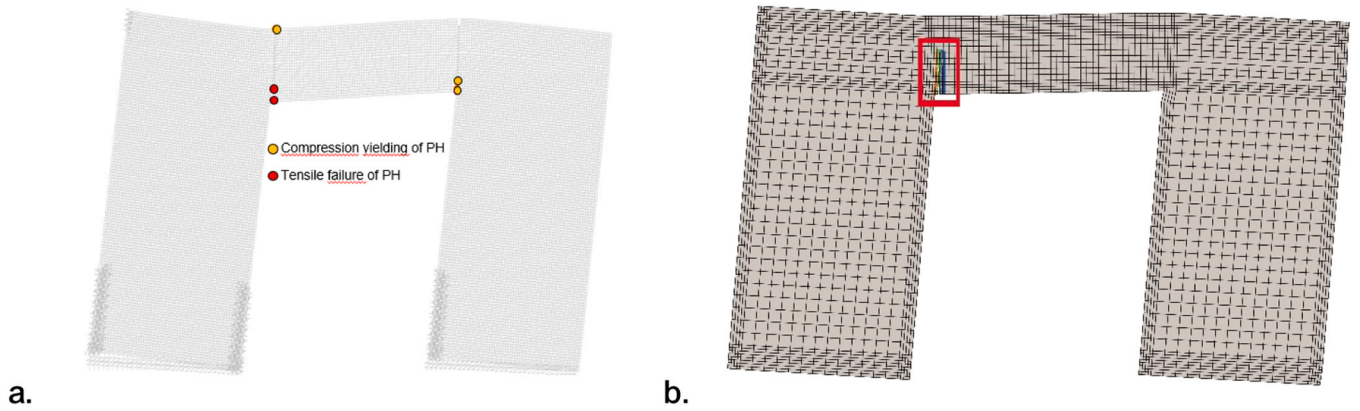

Fig. 11. Numerical models for Wall 01: a) PHM and b) CPEM.

other parameters represent the maximum stress reached at failure.

3.3. Input parameters for the numerical models used for validation

The mechanical properties of the CLT panels used in the numerical models to validate the proposal against the six selected shearwalls with openings are reported in Table 4 in terms of modulus of elasticity parallel to the grain E, shear modulus G as well as axial strength per unit length, $n_{ax,Rd,}$ and shear strength per unit length, $n_{v,Rd}$.

It is noteworthy to highlight that although variable $n_{ax,Rd}$ represents the compressive or tensile forces strength capacity, the flexural strength capacity was used in the determination of strength capacity of the elements because the CLT elements are subjected primarily to bending. As a result, the tensile $n_{ax,t,Rd}$ and compressive $n_{ax,c,Rd}$ axial strengths of the laminations have been replaced with the bending strength, $n_{ax,m,Rd}$, in Eqs. 5 and 6.

Additionally, the numerical model where XFEM is used to predict the crack openings and propagation, the critical values of the energy release needed to describe the fracture criterion were selected to be equal to G_{IC}= 176 N/m and G_{IIC}= 734 N/m. This value is based on experimental evidence presented by Haller and Putzger [49], obtained by performing double cantilever beam fracture tests on spruce, and was also assumed by Kováčiková et al. [39] in their numerical investigation on C24-graded elements.

For parts other than lintels and parapet, the constitutive law is integrated using the Hill yield anisotropic criterion which is able to account for the possible compressive damage [50,51]. Based on the panel orientation, the reference resistance value for compression parallel to grain, $f_{c,0}$, was assumed and the corresponding anisotropic stress ratios (R_{ii} with i = 1,2,3; j = 1,2,3) for the other principal directions of interest were calculated according to Eqs. 18 and 19.

$$R_{ii} = \frac{\overline{\sigma}_{ii}}{\sigma^0} \tag{18}$$

$$R_{ij} = \frac{\overline{\tau}_{ij}}{\sigma^0/\sqrt{3}} \tag{19}$$

where $\overline{\sigma}_{11} = f_{c,0}$, $\overline{\sigma}_{22} = \overline{\sigma}_{33} = f_{c,90}$ and $\overline{\tau}_{12} = \overline{\tau}_{13} = \overline{\tau}_{23} = f_v$ are the measured yield stress value and $\sigma_0 = f_{c,0}$ is the reference yield stress specified for the plasticity definition.

In accordance with Jeleč at al. [52] and Brandner et al. [44], the values assumed for the compression parallel to the grain $f_{c,0}$ and perpendicular to the grain $f_{c,90}$ could be taken as $f_{c,0} = f_m$ and $f_{c,90} = 3MPa$.

The force-displacement curves of the mechanical anchors, adopted in numerical models and obtained from published experimental studies are reproduced in Fig. 9.

3.4. Comparison between numerical models and shearwall tests

The comparison between the proposed numerical models presented in Sections 3.1 and 3.2 and the six experimentally tested shearwalls is shown in Fig. 10 in terms of load-displacement curves. Additionally, a comparison in terms of wall stiffness k (calculated according to procedure reported in EN12512 [54]), maximum forces F_{max}, and failure mode is reported in Table 5, which also includes the percentage difference ε for the stiffness and maximum force. It is noteworthy to mention that for the shearwalls tested by Ceccotti et al. [3], Dujic et al. [4] and Popovski et al. [5], where a cyclic load protocol was adopted, the comparison was conducted in relation to the backbone curve of the first quadrant. In Fig. 11, the deformed shape of Wall 01 corresponding to a value of displacement equal to 25 mm is shown for both the proposed models.

The results show that the prediction of the models is reasonable, and it can be noted that the numerical models were able to not only correctly predict the elastic behaviour of the shearwalls but also reasonably estimate the inelastic behaviour after the yielding of the mechanical anchors or crack openings in the CLT panels. For all six shearwalls, the models were also able to appropriately predict the failure mode

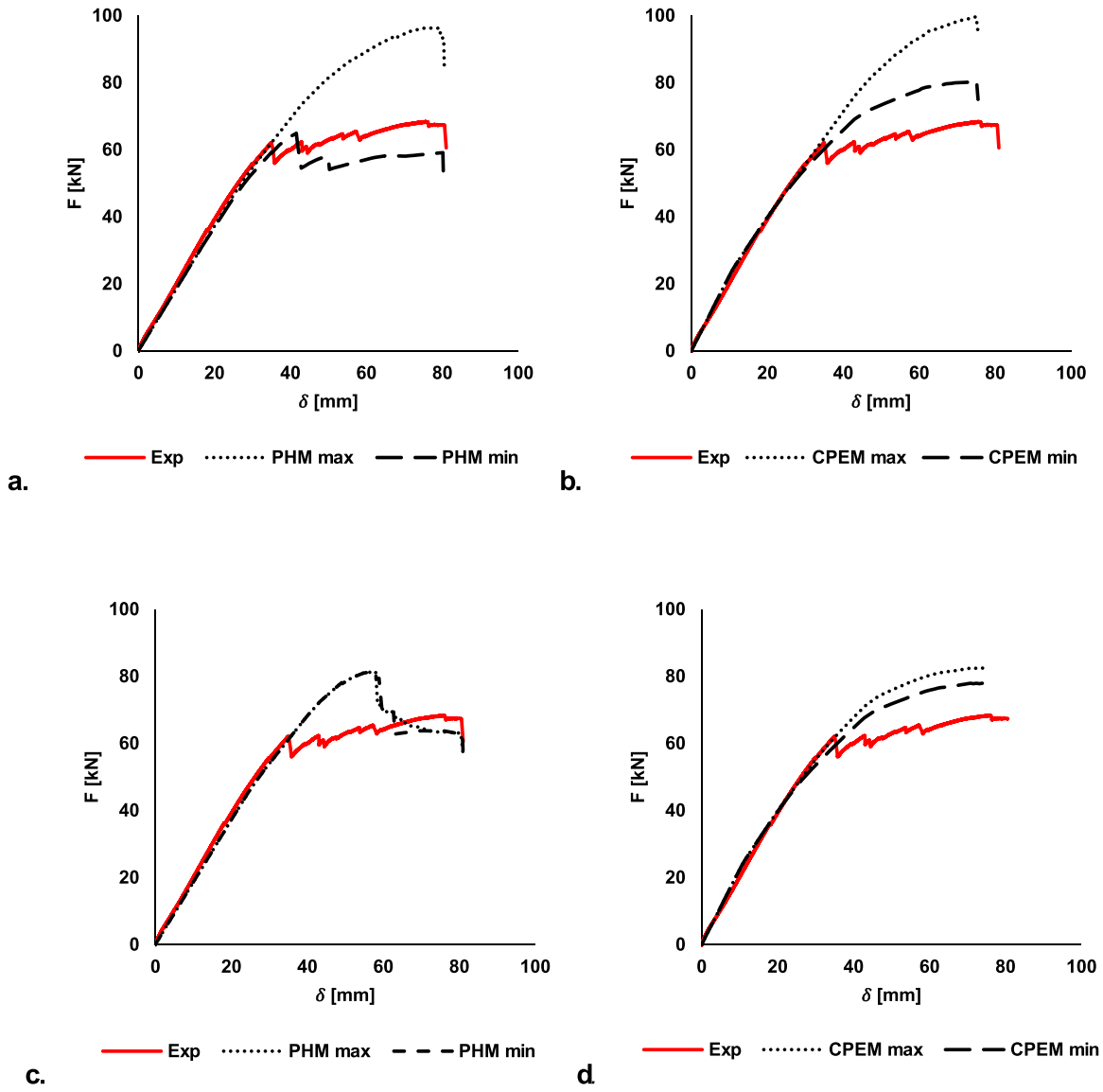

Fig. 12. Comparison between experimental test on Wall 06 and numerical model: a) PHM and b) CPEM with maximum and minimum values of bending strength for CLT beam; c) PHM and b) CPEM with maximum and minimum value of shear strength for unit length.

observed in the tests (see Table 5).

An exception to this general fit is the results obtained from the comparison between the proposed models and the shearwall tested by Mestar et al. [9]. In this example, the numerical models were able to accurately predict the stiffness and ultimate displacement but not the maximum force. Such discrepancy in terms of maximum force can be attributed to the high variability associated with the strength of CLT panels also observed in CLT beam tests. To illustrate this hypothesis, the average values obtained from the beam tests were replaced in the numerical model with the maximum and minimum bending strength values obtained from beam tests, as shown in Fig. 12 (a-b). The figure clearly demonstrates the sensitivity of the model to the strength of the CLT panel, where the model with the maximum or average strength values was not capable of accurately predict the behaviour post crack opening of the shearwall tested by Mestar et al. [9]. Further numerical analyses were carried out by fixing the average value of bending strength and varying the shear strength between the maximum and minimum values per unit length obtained from beam tests, as shown in Fig. 12 (c-d). In both numerical models, the difference between the obtained curves is negligible. This panel seems to have a relatively low strength and this particularity was captured by the model when the minimum strength obtained from beam tests was used. Selecting the minimum strength caused the lintel to fail earlier and provided a behaviour that was consistent with that observed in the test, whereas selecting the maximum strength resulted in an ultimate failure in the hold-down, which was inconsistent with the experimental observations, as shown in Fig. 12. This observation presents an important question regarding model inputs, which is raised here but further investigation of this issues was deemed to be beyond the scope of the current paper.

In general, relatively small differences can be observed between the two proposed models in terms of general behaviour trends, with the exception of Wall 06, for a similar reason provided regarding strength input for the CLT panel which affects the models' abilities to predict the behaviour of the wall post crack opening.

4. Comparison between the proposed numerical models and models with elastic behaviour of CLT panels

In order to highlight the differences and potential benefits obtained by adopting numerical models capable of considering the non-linear behaviour of the CLT panel, a comparison between the two proposed procedures and a model assuming linear-elastic behaviour of CLT panels

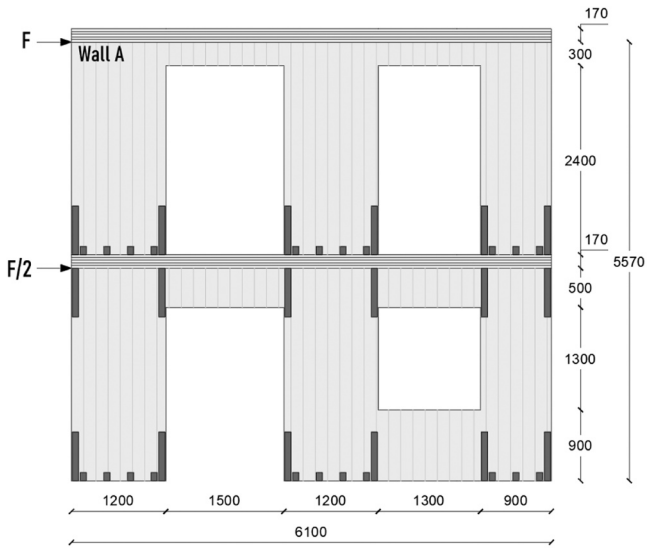

Fig. 13. The two storey shearwall analysed for the comparison (dimensions in mm).

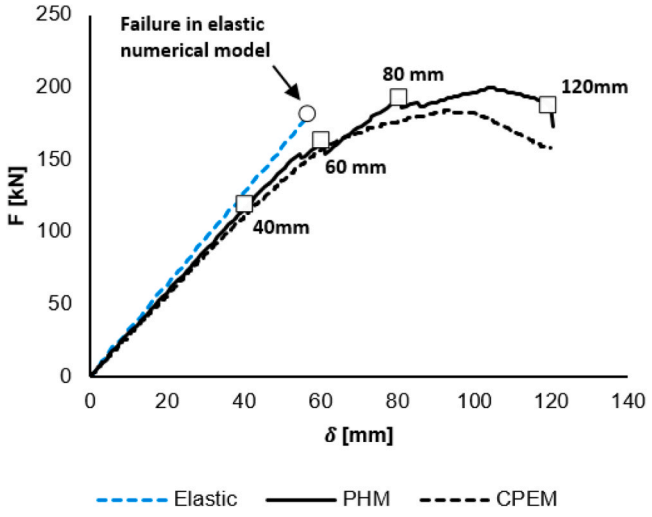

Fig. 14. Base shear-displacement curves obtained from elastic, PHM and CPEM model.

is undertaken.

For both models (PHM and CPEM), the geometrical dimensions, the distribution of horizontal loads along the height of the shearwall as well as the layout of mechanical anchors are reported in Fig. 13. CLT panels consisting of 3-ply 90 mm thick boards (30v-30 h-30v) were selected. A vertical load equal to 15 kN/m was applied at each storey. The mechanical properties of Wall 01, reported in Table 4, were adopted for the CLT laminations. The shear walls are anchored using ABR105 angle brackets spaced at 300 mm and WHT620 hold-downs placed at each end of wall segments. The angle brackets are connected to the CLT panel using ten 4,2x89mm spiral nails and the hold-downs are attached to the panels using fifty-five 4x60mm ring shanked nails. The same mechanical behaviours of the anchors, as those depicted in Fig. 9, were used. It is noteworthy to mention that the interaction between shear-walls and floor diaphragms was not considered in the model and is outside the scope of this study.

The comparisons were performed in terms of force-displacement curves, as shown in Fig. 14, stiffness k, maximum base shear V_{max}, and ultimate displacement, δ_u, at the top of the shearwalls, as reported in Tables 6 and 7.

From the comparison carried out with the PHM model (Table 6), it can be observed that the discrepancy between the proposed models and the model with an elastic behaviour of CLT panels is not significant in terms of stiffness and maximum base shear (maximum of 10 % difference). A greater difference is observed, however, in terms of post peak behaviour, represented by the 111 % difference in terms of ultimate displacement. The elastic model is clearly not capable of predicting the mechanical behaviour of the shearwall after the crack opening, and the load-displacement curve was thus terminated much earlier than the

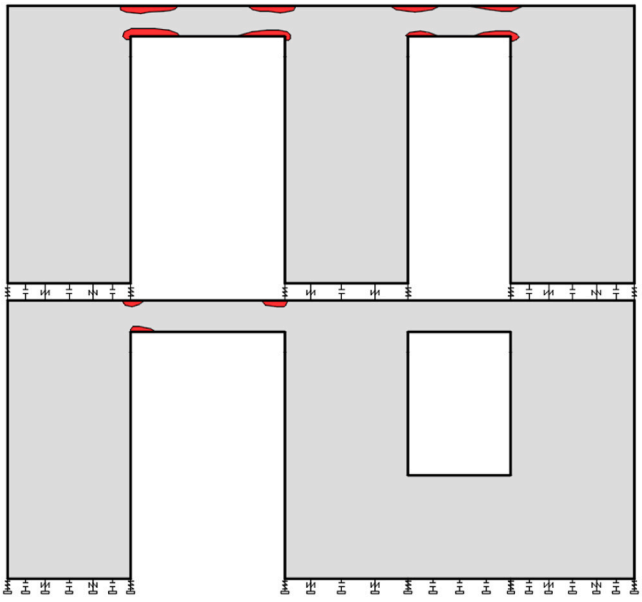

Fig. 15. Zones where the in-plane axial strength were attained in the PHM elastic model.

Table 6
Comparison in terms of stiffness, maximum base shear and ultimate displacement between the elastic and the model with plastic hinges.

k [kN/mm]			V_{max} [kN]			δ_u [mm]			Ultimate condition	
Elastic	PHM	ε_{PHM}	Elastic	PHM	ε_{PHM}	Elastic	PHM	ε_{PHM}	Elastic	PHM
3,2	2,9	−8,5 %	181,7	199,5	10,0 %	57,0	120,4	111,2 %	CLT panel	Hold-down

Table 7
Comparison in terms of stiffness, maximum base shear and ultimate displacement between the elastic and the CPEM model.

k [kN/mm]			V_{max} [kN]			δ_u [mm]			Ultimate condition	
Elastic	CPEM	ε_{CPEM}	Elastic	CPEM	ε_{CPEM}	Elastic	CPEM	ε_{CPEM}	Elastic	CPEM
3,2	2,8	−12,5 %	181,7	183,8	1,2 %	57,0	119,9	110,4 %	CLT panel	Hold-down

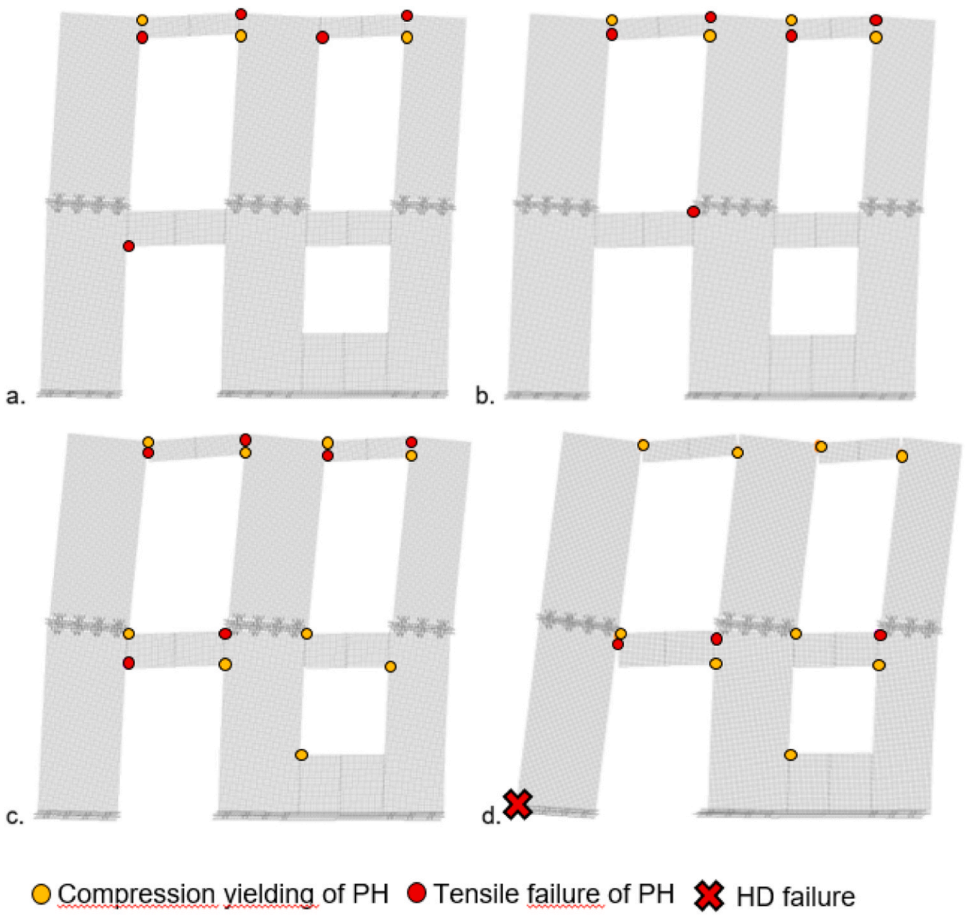

Fig. 16. Evolution of crack opening at a) 40 mm (I), b) 60 mm (II), c) 80 mm (III), d) 120 mm (IV) displacement.

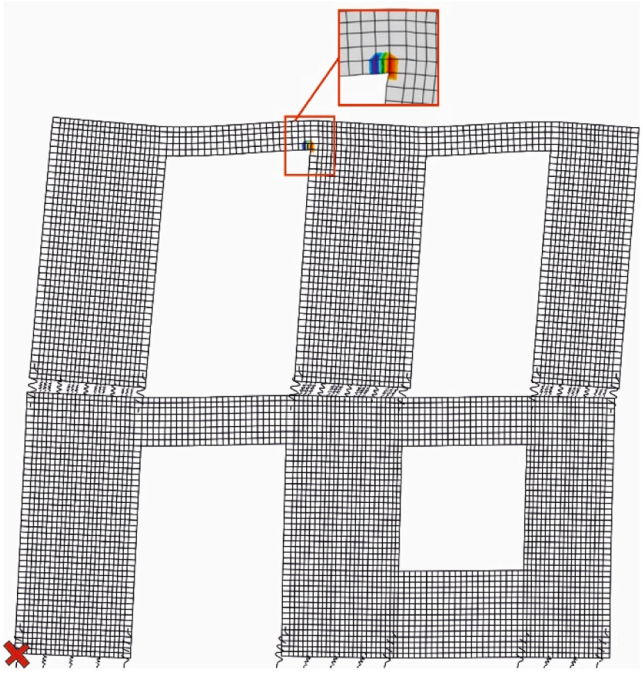

Fig. 17. Crack opening in CPEM model at a120mm of displacement.

value of displacement obtained from the proposed models. A correct prediction of ultimate displacement is essential, especially in seismic analyses where the deformation capacity of structural systems needs to be determined.

Fig. 15 shows the zones where the in-plane axial strength was attained in the elastic model, corresponding to the bending failure condition of lintels in the CLT panels and to a displacement at the top of the second storey equal to 57 mm. The failure condition in the elastic model was determined by means of a step-by-step verification of the internal forces in all shell elements to confirm occurrence of possible failure. No yielding in the connections was detected at this level of displacement. From the comparison between the CPEM and model with an elastic behaviour of CLT panels, it can be observed that the absolute discrepancy in terms of elastic stiffness (12,5 %) and maximum base shear (1,2 %) is relatively insignificant, as reported in Table 7. As for the PHM model, a significant difference is conversely observed in terms of ultimate displacement (110 %).

Fig. 16 shows the activation of different plastic hinges in the wall for the PHM model, due to the attainment of axial strength capacity, and the propagation of cracks in the lintel beams in both storeys for different values of top shearwall displacement. It can be observed that cracks initiate at the bottom corners of lintel beams at the second storey (Fig. 16a) and propagate to the top corners of the same lintels (Fig. 16b). Increasing the shearwall lateral displacement results in crack openings at the lintel beams of the first storey, whereas at the second storey lintel beams are only connected to the wall segments by a truss element (Fig. 16c). The failure condition, shown in Fig. 16d, refers to reaching the ultimate displacement in the hold-down at the first storey. Fig. 17 shows the failure condition in the CPEM model.

This investigation highlights the important contribution of lintel

beams, and shows that when a flexural crack forms at the interface between the lintel beam and the wall, the crack does not necessarily cause ultimate failure to occur but rather a redistribution of stresses in the lintel beam, which maintains some degree of coupling between the vertical wall segments. The coupling mechanism is not present to the same degree when shear failure occurs due to the significant strength degradation in the lintel and diminishment of continuity between the elements. Also, the number of layers (e.g. 3- and 5-ply), and possibly their orientation, may be a parameter of importance to be considered in the analysis of the redistribution of stresses in the lintel beams. This observation raises an important issue that should be the subject of further investigations. These findings could have significant implications on the way CLT shearwalls with openings are analyzed and designed. It suggests that by considering the initial crack opening to be representative of the ultimate failure of the wall, and employing linear elastic modeling assumptions to predict such failure, may be excessively conservative. A consideration of the stress redistribution near crack openings and the subsequent inelastic behaviour should be taken into account in the analysis in order to capture the actual inelastic behaviour of the CLT shearwall.

5. Conclusions

In this paper, two proposals for the numerical prediction of the mechanical behaviour of CLT shearwalls with cut openings capable of considering the non-linear behaviour of CLT panels beyond crack opening, are presented. The proposed numerical models were validated using experimental results obtained from six full-scale shearwalls in the literature. A comparison between the two models revealed relatively small differences in terms of general behaviour trends. The results of the comparison with the experimental results showed the ability of the models not only to predict the elastic behaviour of the shearwalls but also the inelastic behaviour after the yielding of the mechanical anchors or crack openings in the CLT panels. The analyses showed a high sensitivity of the models to the strength of the CLT panel.

The impact and advantages of accurately predicting the non-linear behaviour of the CLT panels were investigated and demonstrated through a numerical analysis of a case-study representing multi-storey shearwall with multiple openings. A comparison between the proposed procedure and a model assuming linear-elastic behaviour of CLT panels showed inability of the elastic model to predict the mechanical behaviour of shearwalls after the crack opening. The findings demonstrated that employing linear elastic modeling assumptions to predict the behaviour of CLT shearwalls with openings may not be adequate. It is therefore suggested that a recognition of the stress redistribution near crack openings and subsequent inelastic behaviour should be considered in the analysis in order to capture the inelastic behaviour in the CLT shearwall.

CRediT authorship contribution statement

Andrea Polastri: Formal analysis, Investigation, Supervision. **Daniele Casagrande:** Conceptualization, Funding acquisition, Methodology, Resources, Supervision, Writing – original draft, Writing – review & editing. **Ghasan Doudak:** Methodology, Supervision, Writing – original draft, Writing – review & editing. **Martina Sciomenta:** Data curation, Formal analysis, Software, Writing – original draft, Writing – review & editing, Validation. **Riccardo Fanti:** Conceptualization, Data curation, Formal analysis, Methodology, Software, Validation, Writing – original draft, Writing – review & editing.

Acknowledgments

The authors would like to acknowledge Dr. Eng. Igor Gavrić for his valuable input and clarification on the results obtained from his experimental tests reported in literature. A special thank to Diego Magnago (CNR-IBE San Michele all'Adige - Mechanical Test Laboratory) for running all tests on CLT beams. Dr. Daniele Casagrande also acknowledges the Italian Ministry of Universities and Research 378 (MUR), in the framework of the project DICAM-EXC (Departments of Excellence 2023–2027, grant L232/2016).

References

[1] Li M, Lam F. Lateral behaviour of cross laminated timber shear walls under reversed cyclic loads. : Tenth Pac Conf Earthq Eng Syd: Aust 2015.
[2] Gavric I, Fragiacomo M, Ceccotti A. Cyclic behavior of CLT wall systems: experimental tests and analytical prediction models. Am Soc Civ Eng J Struct Eng 2015;141(11). https://doi.org/10.1061/(ASCE)ST.1943-. 541X.0001246.
[3] Ceccotti A, Lauriola M, Pinna M, Sandhaas C. SOFIE project – cyclic tests on crosslaminated wooden panels. : Proc World Conf Timber Eng (WCTE), Portland, OR, USA 2006;vol. 1:805–12.
[4] Dujic B, Klobcar S, Zarnic R. Shear capacity of cross-laminated wooden walls. 10th World Conf Timber Eng 2008 2008;3:1641–8. ISBN: 978-161567088-8.
[5] Popovski, M., Schneider, J., Schweinsteiger, M. Lateral load resistance of cross-laminated wood panels (2010) 11th World Conference on Timber Engineering 2010, WCTE 2010, 4, pp. 3394–3403. ISBN: 978–162276175-3.
[6] Popovski M, Gavric I, Schneider J. Performance of two-storey CLT house subjected to lateral loads. WCTE 2014 - World Conf Timber Eng, Proc 2014.
[7] Yasumura M, Kobayashi K, Okabe M, Miyake T, Matsumoto K. Full-scale tests and numerical analysis of low-rise CLT structures under lateral loading. J Struct Eng (N Y, NY) 2015;142(4). https://doi.org/10.1061/(ASCE)ST.1943-. 541X.0001348.
[8] Awad V, Giresini L, Koshihara M, Puppio ML, Sassu M. Experimental analysis and numerical models of CLT shear walls under cyclic loading. Intech,; 2017.
[9] Mestar M, Doudak G, Polastri A, Casagrande D. Investigate the kinematic modes of CLT shear-walls with openings. Eng Struct 2021;228:111475.
[10] Casagrande D, Fanti R, Doudak G, Polastrci A. Experimental and numerical study on the mechanical behaviour of CLT shearwalls with openings. Constr Build Mater September 2021;298(6)):123858.
[11] Moosbrugger T, Guggenberger W, Bogensperger T. Crosslaminated timber wall segments under homogeneous shear – with and without openings. Proc World Conf Timber Eng (WCTE), Portland, OR, USA 2006;vol. 1:219–28.
[12] Dujic B, Klobcar S, Zarnic R. Influence of openings on shear capacity of wooden walls. NZ Timb Des J 2015;16(1).
[13] Shahnewaz M, Alam MS, Tannert T, Popovski M. Cross laminated timber walls with openings: inn-plane stiffness prediction and sensitivity analysis. Proceedings of 5th International Structural Specialty Conference, vol. 4. At London, ON, USA: CSCE,; 2016. p. 2943–52.
[14] Fragiacomo M, Dujic B, Sustersic I. Elastic and ductile design of multi-storey crosslam massive wooden buildings under seismic actions. Eng Struct 2011;33(11): 3043–53. https://doi.org/10.1016/j.engstruct.2011.05.020.
[15] Pai SGS, Lam F, Haukaas T. Force transfer around openings in cross-laminated timber shear walls. J Struct Eng 2017;143(4):04016215. https://doi.org/10.1061/(ASCE)ST.1943-541X.0001674.
[16] Casagrande D, Fanti R, Greco M, Gavric I, Polastri A. On the distribution of internal forces in single-storey CLT symmetric shear-walls with openings. Structures 2021; 33:4718–42. https://doi.org/10.1016/j.istruc.2021.06.084.
[17] Khajehpour M, Casagrande D, Doudak D. The role of lintels and parapets on the mechanical performance of multi-storey cross laminated timber shearwalls with openings. Eng Struct 2022;255(2022):113912.
[18] Mestar M, Doudak G, Polastri A, Casagrande D. Investigating the kinematic modes of CLT shear-walls with openings (art. no) Eng Struct 2021;228:111475. https://doi.org/10.1016/j.engstruct.2020.111475.
[19] Casagrande D, Doudak G, Vettori M, Fanti R. Proposal for an equivalent frame model for the analysis of multi-storey monolithic CLT shearwalls (art. no) Eng Struct 2021;245:112894. https://doi.org/10.1016/j.engstruct.2021.112894.
[20] Griffith AA. "The Phenomena of Rupture and Flow in Solids". Trans Roy Soc A221 163-198 Philos Trans R Soc A Math Phys Eng Sci 1921;221(582-593):163–98. https://doi.org/10.1098/rsta.1921.0006.
[21] Irwin GR. "Analysis of Stresses and Strains Near End of a Crack Traversing a Plate". J Appl Mech 1956;24(24).
[22] Rice JR. "Mathematical Analysis in the Mechanics of Fracture" (Mathematical Fundamentals). In: Liebowitz H, editor. Chapter 3 of Fracture: An Advanced Treatise, Vol. 2. N.Y.: Academic Press; 1968. p. 191–311 (Mathematical Fundamentals).
[23] Serrano E, Gustafsson PJ. Fracture mechanics in timber engineering – Strength analyses of components and joints. Mater Struct 2007;40:87–96. https://doi.org/10.1617/s11527-006-9121-0.
[24] Conrad MPC, Smith GD, Fernlund G. Fracture of solid wood: a review of structure and properties at different length scales. Wood and Fiber Science, 35. the Society of Wood Science and Technology,; 2003. p. 570–84.
[25] Jockwer R. Structural behaviour of glued laminated timber beams with unreinforced and reinforced notches, (2014), Published by ETH-Zürich.
[26] Nakao T, Susanti CME, Yoshihara H. Examination of the failure behavior of wood with a short crack in the radial–longitudinal system by single-edge-notched bending test. J Wood Sci 2012;58:453–8. https://doi.org/10.1007/s10086-012-1266-6.
[27] Blackman BRK, Hadavinia H, Kinloch AJ, Williams JG. The use of a cohesive zone model to study the fracture of fibre composites and adhesively-bonded joints. Int J Fract 2003;119:25–46.

[28] Andersson T, Stigh U. The stress-elongation relation for an adhesive layer loaded in peel using equilibrium of energetic forces. Int J Solids Struct 2004;41:413–34.
[29] Schoenmakers JCM. Elementary and advanced modelling of the splitting strength of timber connections. Heron 2008;Vol.1:58–84.
[30] Serrano E., "Adhesive Joints In Timber Engineering - Modelling And Testing Of Fracture Properties" PhD Thesis, Lund University, Department of Mechanics and Materials, (2000) ISRN LUTVDG/TVSM–00/1012–SE (1–173) ISBN 91–7874-095–9 ISSN 0281–6679.
[31] Danielsson H, Gustafsson PJ. A three dimensional plasticity model for perpendicular to grain cohesive fracture in wood. Eng Fract Mech 2013;98:137–52.
[32] Serrano E, Gustafsson PJ. Infuence of bondline brittleness and defects on the strength of timber finger-joints. Int J Adhes Adhes 1999;19:9–17.
[33] Serrano E. Glued-in rods for timber structures — a 3D model and finite element parameter studies. ISSN 0143-7496 Int J Adhes Adhes 2001;Volume 21(Issue 2): 115–27. https://doi.org/10.1016/S0143-7496(00)00043-9.
[34] Danielsson H, Gustafsson PJ. Fracture analysis of glued laminated timber beams with a hole using a 3D cohesive zone model. ISSN 0013-7944 Eng Fract Mech 2014;Volumes 124–125:182–95. https://doi.org/10.1016/j.engfracmech.2014.04.020.
[35] Lin M, Agbo S, Cheng JJR, Yoosef-Ghodsi N, Adeeb S. "Application of the Extended Finite Element Method (XFEM) to Simulate Crack Propagation in Pressurized Steel Pipes.". V03BT03A024. ASME Proc ASME 2017 Press Vessels Pip Conf Vol 3B: Des Anal Waikoloa, Hawaii, USA 2017. https://doi.org/10.1115/PVP2017-65575.
[36] Ferretti D, Michelini E, Rosati G. Cracking in autoclaved aerated concrete: Experimental investigation and XFEM modeling. Cem Concr Res 2015;Volume 67: 156–67.
[37] Zhao L, Zhi J, Zhang J, Liu Z, Hu N. XFEM simulation of delamination in composite laminates. Compos Part A: Appl Sci Manuf 2016;Volume 80:61–71. https://doi.org/10.1016/j.compositesa.2015.10.007.
[38] Qiu LP, Zhu EC, van de Kuilen JWG. Modeling crack propagation in wood by extended finite element method. Eur J Wood Prod 2014;72:273–83. https://doi.org/10.1007/s00107-013-0773-5.
[39] Kováčiková J, Ivánková O, Berg S, Ekevad M, Klas T. Computational and experimental analysis of timber beams with different types of flaws. AIP Conf Proc 2020;2309:020036. https://doi.org/10.1063/5.0034413.
[40] Tapia C. and Simon S. Applying the XFEM method to the simulation of tensile failure in timber boards and finger-joints in a glulam strength model, Compwood 2019 Vaxjo, Sweeden, ISBN: 978–91-88898–64-7.
[41] Habite, T., Florisson, S., Vessby, J. (2018) Numerical Simulation of Moisture-Induced Crack Propagation in Dowelled Timber Connection Using XFE MIn: 2018 World Conference on Timber Engineering (WCTE), August 20–23, 2018,Seoul, Republic of Korea World Conference on Timber Engineering (WCTE).
[42] Gebhardt C, Kaliske M. An XFEM-approach to model brittle failure of wood. ISSN 0141-0296 Eng Struct 2020;Volume 212:110236. https://doi.org/10.1016/j.engstruct.2020.110236.
[43] Bogensperger T, Moosbrugger T, Silly G. Verification of CLT-Plates under loads in plane. WCTE 2010.
[44] Brandner R, Dietsch P, Droscher J, Schulte-Wrede M, Kreuzinger H, Sieder M. Crosslaminated timber (CLT) diaphragms under shear: Test configuration, properties and design. Constr Build Mater 2017;147:312–27. 2017.
[45] CSI SAP2000 Integrated Software for Structural Analysis and Design (2017). Computers and Structures Inc Berkeley, California
[46] ABAQUS (Version 2023, Dassault Systemes Simulia, Inc)
[47] Shen Y, Schneider J, Tesfamariam S, Stiemer S, Chen Z. Cyclic behavior of bracket connections for cross-laminated timber (CLT): Assessment and comparison of experimental and numerical models studies. J Build Eng 2021;39:102–97.
[48] Andreolli M, Tomasi R, Polastri A. "Experimental investigationon in-plane behaviour of cross-laminated timber elements,". Proc CIB-W18 Växjö 2012.
[49] Haller P, Putzger R. "Fracture Energy in Mode I and Mode II of Reinforced Wood". Proc 2nd Colloq Text Reinf Struct, (Tech Univ Dresd: Eig 2003:247–58. CTRS2.
[50] Sciomenta M, Bedon C, Fragiacomo M, Luongo A. Shear performance assessment of a timber log-house walls under in-plane lateral loads via numerical anda analytical modelling. Buildings 2018;8:99.
[51] Bedon C, Fragiacomo M. Numerical analysis of timber-to-timber joints and composite beams with inclined self-tapping screws. Compos Struct 2019;Vol.207: 13–28.
[52] Jeleč M, Varevac D, Rajčić V. Cross-laminated timber (CLT) – a state of the art report (doi) GRAĐEVINAR 2018;70(2):75–95. https://doi.org/10.14256/JCE.2071.2017.
[53] EN 408 (2003) Timber Structures - Structural Timber and Glued-laminated Timber: Determination of Some Physical and Mechanical Properties. CEN, Brussels, Belgium
[54] EN 12512:2001/A1:2005 (2005). Timber structures—test methods–cyclic Testing of Joints Made with Mechanical Fasteners. CEN, Brussels, Belgium
[55] ETA-Denmark, ETA-11/0086. European technical assessment. Three-dimensional nailing plate (Angle Bracket or Hold Down for timber-to-timber or timber-to-concrete or steel connections), (2015).
[56] ETA-Denmark, ETA-07/0285. European technical assessment. Three-dimensional nailing plate (timber to timber and timber to concrete/steel hold downs and post bases), (2018).
[57] ETA-Denmark, ETA-06/0106. European technical assessment. Three-dimensional nailing plate (timber-to-timber/timber-to-concrete angle bracket), (2021).
[58] OIB-Austrian Institute of Construction Engineering, ETA-06/0138. European technical assessment. Solid wood slab elements to be used as structural elements in buildings, (2021).
[59] Isoda, et al. Experimental Behavior of L-Shaped and T-Shaped Cross-Laminated Timber to Evaluate Shear Walls with Openings. J Struct Eng 2023;Vol. 149(No. 5). https://doi.org/10.1061/JSENDH.STENG-11474.
[60] D'Arenzo G. An elastic model for the prediction of the lateral response of Cross-Laminated Timber shear walls with openings. January 2023 Eng Struct 2023; Volume 274(1):115055. https://doi.org/10.1016/j.engstruct.2022.115055.
[61] Ruggeri EM, D'Arenzo G, Fossetti M. Investigating the effect of the structural interactions due to floors and lintels on the lateral response of multi-storey Cross-Laminated Timber shear walls. Eng Struct 2901 Sept 2023 Artic Number 2023: 116327. https://doi.org/10.1016/j.engstruct.2023.116327.
[62] CLT Handbook, FPInnovation, Canada.
[63] Flaig M, Blass HJ. Shear Strength and Shear Stiffness of CLT-Beams Loaded in Plane. Int Counc Res Innov Build Constr 2013. CIB-W18/46-12-3.
[64] Danielsson H, Serrano E. Cross laminated timber at in-plane beam loading - Prediction of shear stresses in crossing areas. Eng Struct 2018;171:921–7.
[65] Danielsson H, Jeleč M, Serrano E, Rajčić V. Cross laminated timber at in-plane beam loading - Comparison of model predictions and FE-analyses. Eng Struct 2019; 179:246–54 (v).
[66] Danielsson H, Jeleč M. A unified design proposal for shear stress prediction in crossing areas for cross laminated timber at in-plane shear and beam loading conditions. Constr Build Mater 2022;355.